Biointerface Research in Applied Chemistry
Open-Access Journal (ISSN: 2069-5837)

Article
Volume 13, Issue 3, 2023, 216
https://doi.org/10.33263/BRIAC133.216

Study NiO Nanoparticles with Different Surface Morphologies on PET Pyrolysis Kinetic Parameters

Aisha Rashid [1], Salam A. Mohammed [1,*], Hazim F Abbas [1], Mohammed AbdulHakim AlSaadi [2], Noor Ali [1], Noof Khalid [1], Emad Yousif [3], Sausan Alyaqoobi [4], Khamis Al Riami [4]

[1] Department of Chemical and Petrochemical Engineering, College of Engineering and Architecture, University of Nizwa, Sultanate of Oman
[2] National Chair of Materials Science and Metallurgy, University of Nizwa, Sultanate of Oman
[3] Department of Chemistry, College of Science, Al-Nahrain University, Baghdad, Iraq
[4] DARIS Research Centre, University of Nizwa, Sultanate of Oman
* Correspondence: salam.mohammed@unizwa.edu.om (S.A.M.);

Scopus Author ID 57189212521
Received: 2.03.2022; Accepted: 20.04.2022; Published: 5.06.2022

Abstract: Nickle oxide (NiO) nanoparticles have been prepared by chemical method. They were chemically formed using the sol-gel method; the calcination step was carried out using two different environment techniques, the first one an ordinary furnace and a custom-made microwave as a new approach. The synthesized nanoparticles' surface morphology was investigated by scanning electron microscopy (SEM), and transmission electron microscopy (TEM). TGA measured the thermal stability of samples and presented information on NiO nanoparticles.TEM authenticated the formation of nanoparticles with a range between 45 to 95 nm and between 45 and 65 for microwave and furnace samples, respectively. Kinetic study analogy shows the best catalysis found is NiO created by the microwave, where it gave lower activation energy Ea and remaining weight percent. Also, it has a high rate of reaction, especially with PET= 9 mg to NiO=1 mg as the mixing ratio compared to the second type of generated NiO via the ordinary furnace. The microwave calcination step took less than 30 minutes compared to the three hours consumed by the furnace.

Keywords: NPs; microwave; PET; pyrolysis.

1. Introduction

Recently, a dramatic increase in population and lifestyle developments are the main factor in increasing waste production. Therefore, recycling was essential to control waste effectively. It is comprehensively categorized into two classifications fossil-based wastes and bio-based wastes. The main fossil-based waste is Plastic waste, which is considered non-biodegradable and covers large disposal areas. While the production of Bio-based waste has grown because of the utilization of fertilizers and agrochemicals for upgrading crop yield. It is noticeable that biological processes are more qualified for waste form bio-based treating, whereas thermochemical processes are more suitable for treating fossil-based wastes. In nature, fossil-based wastes cannot decay easily, and they need a long time to decompose compared with the fast generation of fossil-based wastes [1-3].

There are various methods to produce biofuel from biomass, which include Gasification, Fermentation, and Pyrolysis. Pyrolysis is the common strategy in biofuel fabrication. Pyrolysis is a promising and eco-friendly process that is a practical option for

forming fuels, chemicals, and hydrogen from biomasses and waste polymers. It is the thermal decomposition process to degrade the polymer of long-chain molecules into smaller or fewer complex molecules under pressure and heat. The process does not involve oxygen, and it needs excessive heat within less time [4,5]. The products of pyrolysis are valuable for industry, particularly refineries and production, which are oil, char, and gas. Numerous specialists picked pyrolysis since the process at a moderate temperature of around 500°C is ready to produce a large amount of liquid oil up to 80% wt. Also, pyrolysis is entirely flexible since the factors of the process can be controlled to improve the product yield dependent on inclinations [1,6].

Waste plastics can be divided into poly (ethylene terephthalate) (PET), polypropylene (PP), polyethylene (PE), poly (vinyl chloride) (PVC), and polystyrene (PS). Polyethylene terephthalate (PET) is a polymer with excessive significance among other plastics globally. It is the most favorable choice for several applications due to its thermoplastic. The consumption of PET increases in industrial innovations and various sectors, resulting in tons of scrap formation in the environment. PET waste rises yearly, creating serious problems for the environment because of its toughness and resilience, and non-degradable nature [2,7-9]. Ranjeet Kumar Mishra *et al*. [10] reported the co-pyrolysis of polyethylene terephthalate (PET) with seeds of Samanea saman (SS) to study the kinetics and synergistic effects between two different feedstocks and concluded that the blending of SS and PET at 3:1 shoes higher synergistic effect and RMS value, therefore, it indicated the maximum formation of hot volatiles during pyrolysis. The analysis of kinetic confirmed that the activation energy (Ea) requirement of individual SS and PET was high in comparison with SS and PET at 3:1 ratio, respectively, which required lower activation energy to start the reaction.

In general, adding the right catalyst will accelerate the pyrolysis chemical reaction with the plastic sample, whereas the catalyst accelerates the chemical reaction but stays unaltered towards the finish of the process. It helps reduce the net emissions of greenhouse gases and the associated volume of waste [11-13]. When the catalyst is utilized, the activation energy of the process is dropped down, hence raising the rate of reaction speed. Catalysts are broadly used to make the best use of the general pyrolysis process proficiency by decreasing operation temperature and time, and working on the quality and quantity of liquid oil through directing specific reactions like aromatic compounds formation, cyclic, oligomerization, cracking, and isomerization reaction [14-16]. This is essential since the process of pyrolysis involves high energy that upsets its business application. The catalyst utilization might help provide energy, as heat is one of the most critical factors in manufacturing.

On the other hand, Zi-Ming Qin *et al*. [17] investigated the catalytic impact of titanium dioxide (TiO_2) filler (anatase type) in decreasing the consumption of energy during silicones pyrolysis. They concluded that the used metal oxide has behaved as remarkably accelerator polysiloxane pyrolysis, which amazingly diminished the temperature of pyrolysis up to 50°C. The remaining residue from the pyrolysis reaction (solid phase) did not contain any siloxanes: $C_6H_{18}O_3Si_3$ (11%), $C_8H_{24}O_4Si_4$ (85%), and $C_{10}H_{30}O_5Si_5$ (4%). The catalyst can be utilized again after reprocessing. Mixing TiO_2 with polysiloxane may turn into a promising innovation for a modest, high efficient, and maintainable component in feedstock reusing polysiloxane.

Dineshkumar M. *et al*. [18] studied biochar produced from senna pendula seedcake using a microwave pyrolysis reactor. The pyrolysis process began from the temperature of 35 to 450°C under a nitrogen atmosphere with a heating rate of 10°C /min and 45 min as residence time. The biochar produced from the pyrolysis is then exposed to sulphonation using fuming sulphuric acid. Pyrolysis happened between 200 and 450°C, as shown in TG analysis, and FTIR

analysis results illustrate that the biochar has been emphatically carbonized upon sulphonation. This study provided a hopeful method for producing effective and inexpensive carbon-based catalysts from biomass waste char.

1.2. Nanostructured.

Metal nanoparticles with ideal surface structure, higher surface area, and explicit optical, attractive, mechanical, and electrical properties drew in a few analysts for achieving extremely good electrochemical performance. The electrochemical process includes the surface or interfaces physical interaction and chemical reaction; therefore, the specified properties play a significant role. The dimension of nanoparticles offers a huge surface area for faradaic reaction and little distance for mass, heat, and charge transfer. Transition metal oxide shows a great hypothetical and is economical with excessive wealth and little poisonousness. A few metal oxides have been reported their efficiency in electrochemical such as manganese, ruthenium, cobalt, tin, nickel oxides, and ferrous oxide [19]. Among other transition metal oxide, Nickel oxide (NiO) has shown great electrochemical effecting and has acquired significant consideration lately because of its properties (optical, mechanical, magnetic, and electronic) and has been accounted as a key factor. Nickel oxide (NiO) has high chemically attractive and stabile properties of physical since it has a stable cubic construction and in a visible wavelength range, has poor absorption bands because of their uncommon properties, which are fairly not normal; it has a wide inborn direct bandgap over 3.2 eV and around 106 Ω.cm as recorded resistance of at room temperature [16,20].

Nanoparticles have arisen as an interesting field of popular materials for a scope of applied applications. Generally, materials are classified as nano when their size or one of their aspects is in the range of 1 to 100 nm. Nanomaterials can improve physical and chemical properties. Those particles' physical and chemical properties rely on their precise structure, shape, and size [17,21].

This technique is not concentrated only on reducing the size but also on expanding the effectiveness of materials. Nanotechnology demonstrated that by producing smaller, faster, lighter, and cheaper devices with more prominent usefulness while utilizing less unrefined components and devouring less energy [22-27]. Nanotechnology applications and products utilize qualities in the transition between the atomic and mesoscopic scales. In other words, nanoscale particles can have diverse Physico-chemical properties concerning microscale or macroscale particles of a similar material reported by Mohammad-Saeed Safdaria *et al*. [27].

There are several techniques to synthesize nanoparticles, which formulate their physiochemical and electrochemical properties. For example, sol–gel method is a wet-chemical method that is widely utilized for the advancement of nanomaterial creatable. This method is utilized for the advancement of different sorts of high-quality metal-based nanomaterials. This strategy is known as a sol-gel technique, as during the synthesis of the metal-oxide nanoparticles, the liquid forerunner is changed to a sol. Sol is progressive gelation followed by elimination of solvent. It is an extremely valuable and simple technique to deliver nanostructures wherein precursors are homogeneously blended in solvent to frame a coordinated nonstop network of the liquid stage (gel) which are then dried and calcinated at various temperatures to form nanoparticles, controlling its morphology, shape, and size. The elements that influence the result from the sol-gel strategy are the precursor nature, hydrolysis rate, aging time, pH, and molar ratio among H_2O and the precursor. The sol-gel strategy is monetarily cordial and enjoys numerous benefits. For example, the delivered material is

homogeneous, the handling temperature is low, and the technique is a simple method to generate composites and complex nanostructures [14,19,21,28-30]. Hany M. Abd El-Lateef *et al*. [22] investigated NiO-nanoparticles that were chemically planned through the surfactant-assisted sol-gel technique. The as-prepared NPs showed electrocatalytic oxidation enhanced urea at different urea doses from 0.01 to 2.0 mol/l. The excellent activity of electrocatalytic could be related to identifying with the fruitful synthesis of NiO-NPs, which can easily form NiOH and produce electrons from urea bonds during the process of electrochemical. Besides, dye-sensitized solar cells and solar-driven and water evaporation are the applications of NiO-NPs production.

The present study aimed to produce nanocatalyst using the sol-gel method and then expose it to high temperature using a furnace and microwave as two different calcination techniques. This article provides a more clear understanding of the pyrolysis of this plastic waste through kinetic and thermodynamic parameter evaluation in addition to the reaction mechanism of the process. At the end, compares the data from each catalyst.

2. Materials and Methods

2.1. Nanocatalyst creation using sol-gel preparation.

To prepare nano NiO using the sol-gel method, 1.2 g of Nickel Nitrate Hexahydrate [$Ni(NO_3)_2$. $6H_2O$] as a solute was placed in 60 ml of ethanol as a solvent, and the PH of the solution was controlled at 2.7. The solution was placed and heated to 60℃ via a magnetic stirrer heater for three hours until the solution became homogeneous and thicker. The solution was divided into two parts, and each one was poured into a beaker and dried for 3 days at room temperature—next, two methods for ordinary furnace and special custom microwave calcination. The first sample was entered into the furnace at a temperature of 500℃ for 3 hours, while the other sample was placed in the microwave at 500 ℃ for half an hour. The generated nano NiO were collected for further experiments.

2.2. TGA (thermogravimetric test).

Two types of samples were prepared by mixed PET with the first kind NiO (microwave) while the other sample was mixed PET prepared the other sample with second kind NiO (furnace). Those samples were introduced in the TGA test under the N2 atmosphere. The process was divided into three parts of the experiment. In the first part, the composition of Nickel Oxide (NiO) with PET was constant, 9 mg of PET and 1 mg of NiO (9:1 ratio). The experiments were conducted at heating rates of 5,10,15, and 20 °C/min to scan the samples in the temperature range of 25°C to 600°C. In the second part, the temperature range was fixed and a 10 °C /min heating rate. The loaded NiO was vertical (0.5, 1, 1.5, 2) mg (Table 1). Only NiO catalyst was used in the third set, about 10 mg within 10/min heating flow rate. The collected data from the mentioned earlier experiment were used for nano data analysis and calculation, such as reaction time, temperature, weight %, heat flow%, and derivatives weight%.

The samples are divided into two sets: Sample 1: PET mixed with NiO in the microwave; Sample 2: PET mixed with NiO in Furnace. The below table presents each composition test.

Table 1. The PET mass to loaded NiO catalysis in mg.

PET(mg)	NiO Cat.(mg)
9	1
8	2
8.5	1.5
9.5	0.5

2.3. Catalyst characterization techniques.

Scanning electron microscopy (SEM) was carried out on Jeol, JSM-651LA (Japan). It is a versatile and powerful tool for material characterization. It becomes more useful and necessary due to the continuous shrinking of the 'material's dimension to determine pore, pore size, and other morphological studies. It is used to know morphological studies of nanoparticles. Energy-dispersive X-ray spectroscopy (EDS) is used to obtain the elemental composition of bulk material or a particular area of that material. A transmutation electron microscope (TEM) image was taken using a JEM-1400 (Jeol, Japan) with an accelerating voltage of 100 kV. It is a device that uses an electron beam to shoot a nanoparticle sample, providing a high-resolution comparison to the other technologies used for light-based shooting. TEM is the best method to measure nanoparticle size, grain size, and morphology directly.

3. Results and Discussion

3.1. Formed nanocatalysts characterization analysis.

The morphology of the nanoparticle is shown in the Figure below. From the images, obviously, the particles were exceptionally agglomerated in nature. Some larger particles are appeared due to aggregating or overlapping of smaller particles. In Figure 1, the SEM pictures show that the homogeneous square-shaped particles and grains are randomly distributed in smaller sizes. While the nanoparticles formed using the furnace have a spherical shape as in Figure 2, and as magnification increases, the more nanoparticle clear.

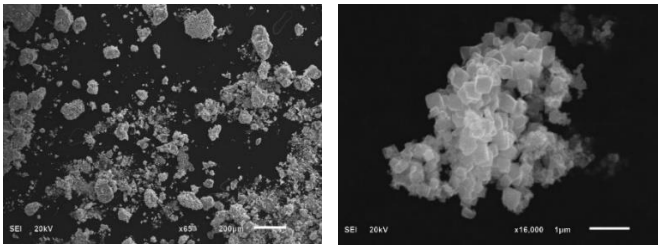

Figure 1. SEM images of NiO nanoparticles by microwave at 500^{o}C for 45min.

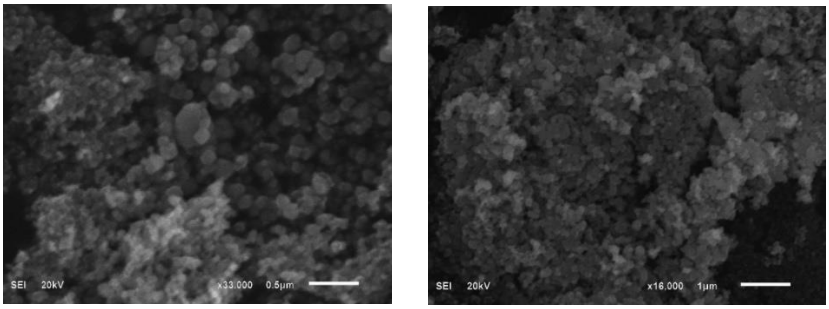

Figure 2. SEM images of NiO nanoparticles calcinated by a furnace at 500 for 3h.

All elements present in NiO nanoparticles were identified and quantified by EDS. The results are demonstrated in Figure 3. It is clear that sample 1 has a higher percentage of Ni than sample 2. The nanoparticle of NiO for sample 1 has 80 % nickel element and 20 % oxygen

element, whereas for sample 2 the nickel element is lower by 10% than the nickel of sample 1. This is a result of exposure to high temperatures in a short time. The calcination step took only 18 minutes to be completed inside the microwave compared to three hours inside the ordinary furnace.

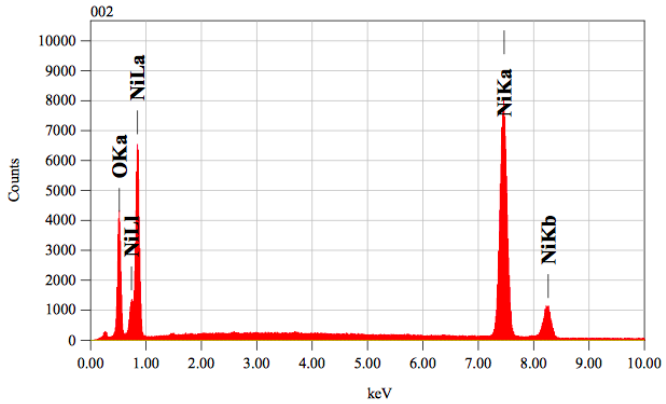

(a)

Element	(Mass%)	(At%)
O K	6.34	19.89
Ni K	93.66	80.11

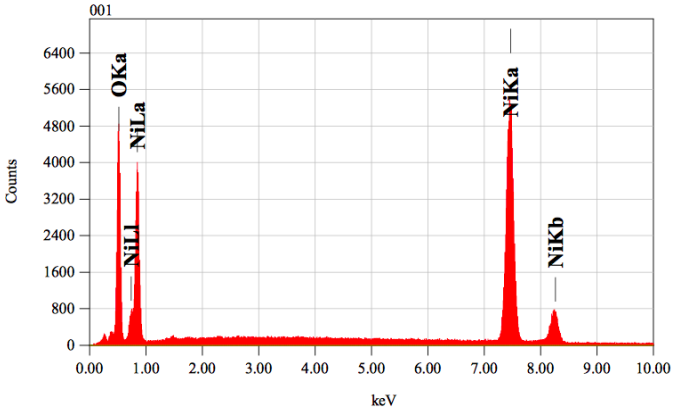

(b)

Element	(Mass%)	(At%)
O K	10.44	29.94
Ni K	79.56	70.06

Figure 3. EDS results of the NiO nanoparticle (a) by microwave and (b) by the furnace.

TEM images demonstrate spherical-shaped NiO nanoparticles in Figure 4 & Figure 5. The aggregated particles are mostly presented. The agglomeration of nanoparticles could be ascribed to their tiny dimensions with high surface energy during the drying step of the sol-gel process. The measured range for the particle sizes was between 45 to 95 nm for sample 1 and between 45 and 65 nm for sample 2.

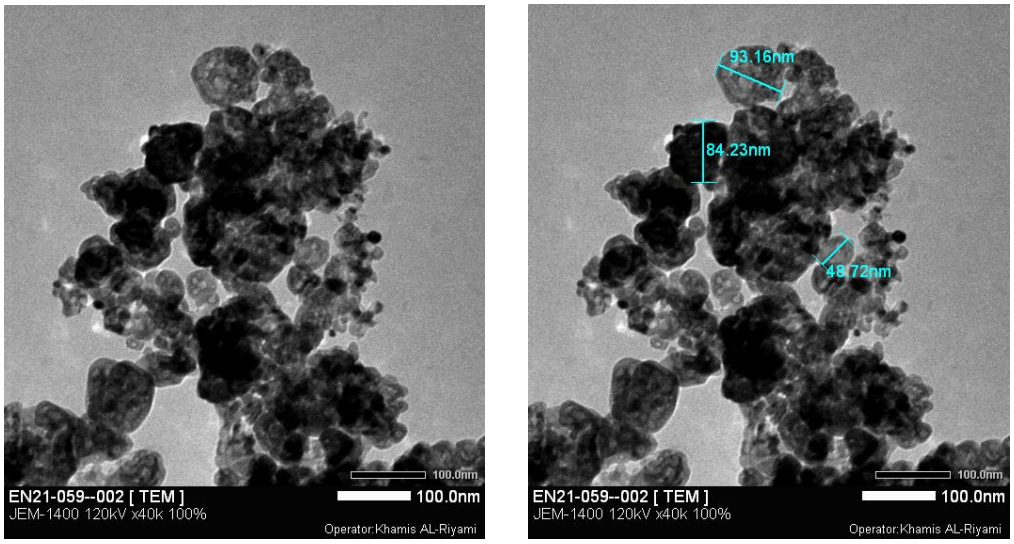

Figure 4. TEM image of NiO nanoparticles by microwave.

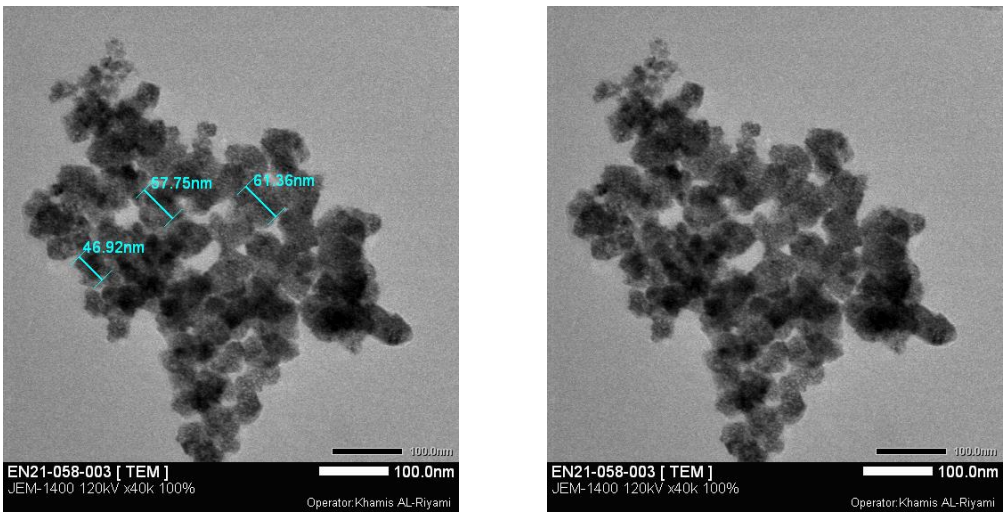

Figure 5. TEM images of NiO nanoparticles by the furnace.

3.2. Weight loss trend.

TGA weight loss data for samples 1 and 2 were obtained under inert (N_2). The percentage of PET sample weight losses plotted with temperature is shown in Figure 6. From TGA analysis (Figure 5), it can be observed that PET decomposition started at around 365 °C and completed at about 470°C. When thermal degradation occurs under an inert environment, the degradation reaction is cased at a residue accumulation of 5% because the volatile matter was thermally decomposed at the temperature range 300-600°C.

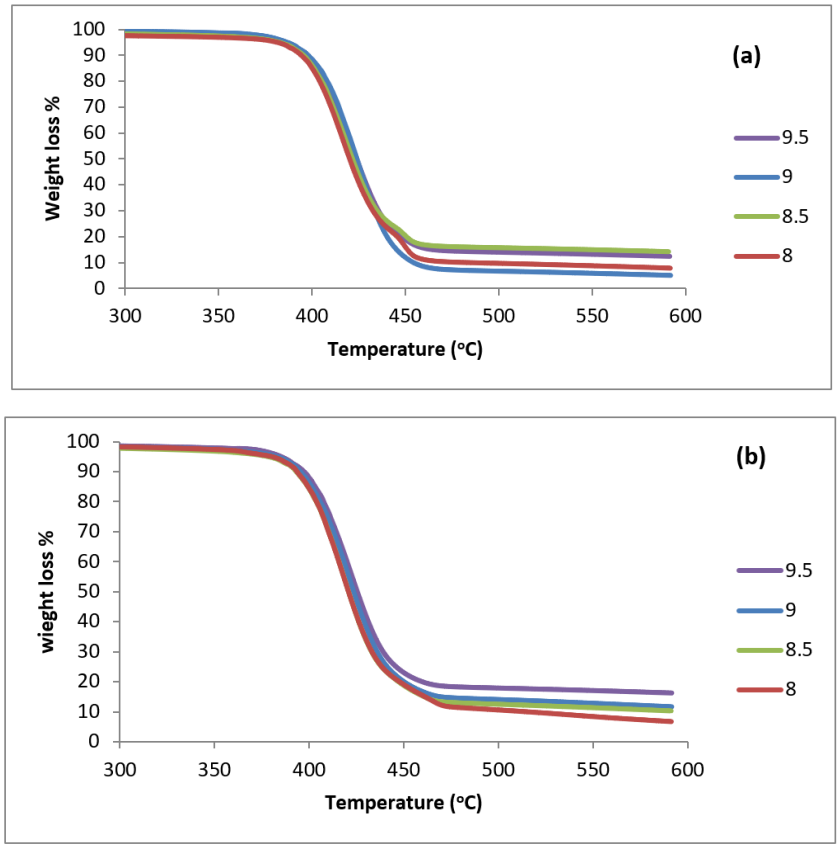

Figure 6. Thermogravimetric curves for (a) sample 1 and (b) sample 2.

As a general observation from Figure 6, three levels as heat trends for the pyrolysis reactions. Figure 6 (a) indicates the first stage of PET/NiO pyrolysis for sample 1 was in the

range of room temperature to 365 °C, reflecting evaporation of the moisture contained, whereby most of the organic compounds were thermally degraded within the samples were. Moreover, the following second PET/NiO pyrolysis level in sample 1 was from 365 °C to 468°C. The decomposition stopped, and the curve stabilized between 450 and 600°C. However, comparing sample 2 with the previous sample in Figure 6 (b), The first step in sample 2 was in the room temperature range of 372 °C. The second stage was 372 °C to 453 °C, which happened faster than sample 1 by 10 degrees. The thermal degradation curve of sample 2 was almost stabilized and formed carbon char in the same temperature range (450 –600 °C).

It is noticeable that PET = 9 has the highest decomposition rate (19.7%/min) than others, whereas the remaining percent of PET (Table 2) is around 5% which is the lowest, around 381.7℃. In contrast, PET =9 of sample 2 has a very high residual weight percent (11.7%) ed to sample 1 and a lower reacting rate (Table 3). Also, PET=8 mg has the lowest percentage of remaining weight at the end of the reaction, which is about 7%. TGA studies clearly show the necessity of high-temperature requirements for pyrolyzing the samples. The weight loss rate of sample 2 is near 17%, whereas the PET=8 has around 16%, and it is acceptable as in Table 3. The onset temperature at 5% conversion of sample 2 (378°C) is lower than sample 1.

Table 2. Main parameters for various amounts of PET in Sample 1.

PET(mg)	onset Temp. at 5% Conversion	Initial reaction rate, Ro	Remaining weight loss %	Max derivative weight (%/min)
9.5	381.7	0.801	12.4	18.6
9	386	0.763	5.1	19.7
8.5	378.5	0.841	14.2	16.9
8	379.2	1.084	7.8	16.3

Table 3. Main parameters for various amounts of PET in Sample 2.

PET(mg)	Onset Temp. at 5% Conversion	Initial reaction rate, Ro	Remaining weight lose %	Max derivative weight (%/min)
9.5	382	0.829	16.3	17.5
9	379.9	0.836	11.7	17.5
8.5	374.2	1.054	10.3	16.8
8	378	0.754	6.7	15.6

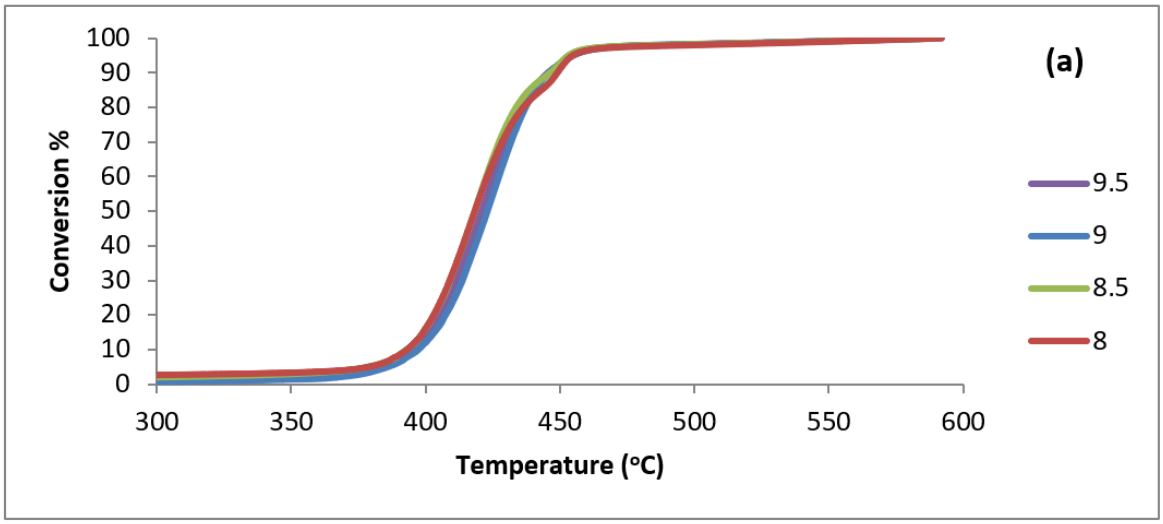

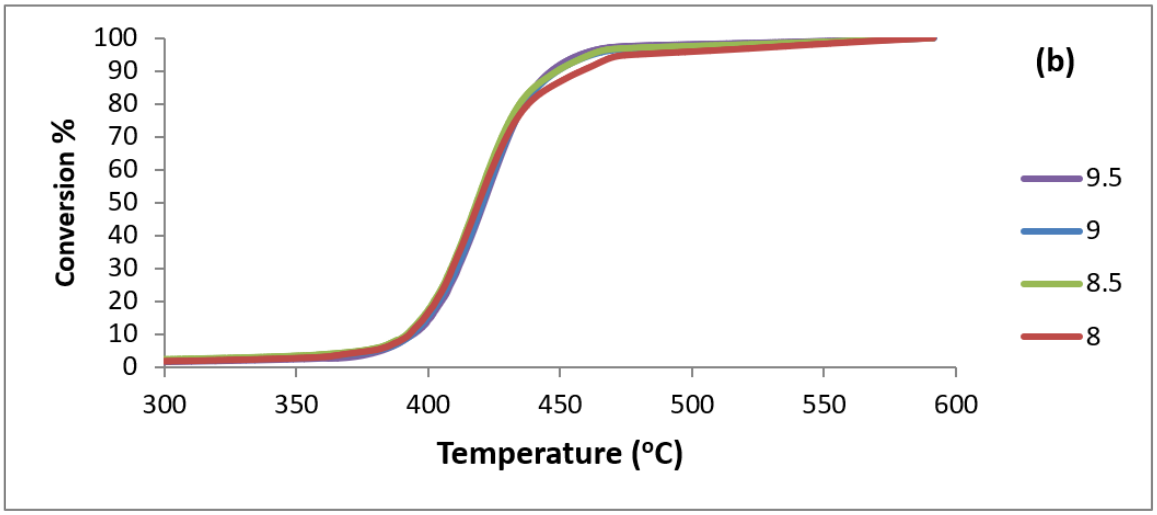

Figure 7. Conversion vs. temperature curves of (a) sample1 and (b) sample 2.

The thermo-gravimetric tests were non-isothermal at four different compositions (9.5, 9, 8.5, and 8 mg) in an N_2 atmosphere with a fixed heating rate of 10 ℃/min shown in Figure 7. Figure 7 demonstrates the conversion results as a function of temperature. It notes that the four samples go in the same direction as one line, considering that they have high thermal stability during the reaction. Sample 2 demonstrates that rising temperature increases follow an increase in the conversion percentage, as in Figure 7 (b). Between 450 and 480 (Figure 7 (b)), PET=8mg has higher conversion than others because most plastic samples are consumed quickly.

The focus of the present study has been using an iso-conversional kinetic model proposed by Flynn-Wall-Ozawa (FWO). This method can be determined the activation energy values for the degradation process without any knowledge of the reaction mechanisms. This is defined by Equation 1 [31]:

$$\log \beta = \log\left[\frac{AF_a}{g(a)R}\right] - 2.315 - 0.4567\frac{E_a}{RT} \qquad \text{Equation 1}$$

Where: β is the heating rate, A is the pre-exponential factor, g(α) is a function of the conversion, E a is the activation energy, and R is the gas constant.

Equation 3.1 is a linear equation, which used to obtain the slope and fined the activation energy as expressed:

$$Ea = (Slope * R)/(-0.4567) \qquad \text{Equation 2}$$

The conversion rate α is defined as:

$$\alpha = \frac{m_0 - m_t}{m_0 - m_f} \qquad \text{Equation 3}$$

Where: m_0 is the initial weight of the sample, m_f is the final weight, and mt is the sample's weight at time (t).

To calculate the remaining weight of PET at the time (mt),

Weight % = Remaining / initial weight =[mt+ Cat. weight/ m0+ Cat. Weight]*100

Then,

$$m_t = [\text{Weight \%} * (\text{m0} + \text{Cat. Weight}) /100] - \text{Cat. weight}$$

where: Cat. weight= catalyst weight

Two types of catalysis are examined under the same conditions: Nickel oxide formed by furnace and microwave. Iso –conversion method proposed by Flynn-Wall-Qzawa (FWO) is used to calculate the kinetic parameters by plotting the natural logarithm of the heating rate in (℃/min) against the inverse of the temperature (*1/k*) where get a linear relationship, as shown in Figure 8. The Ea is obtained from the slope of the straight line.

Table 4 showed a variation of Ea during the reaction progress in the range of 177 – 216.5 (kJ/mol), where 0.9 conversions were eliminated because of extremely high activation energy get compared to the other data. The mean energy of this sample is 195.7 kJ/mol with a standard deviation (STDEVA) of around 12. The E_a gradually increases as conversion rises. On the other hand, the range of E_a for sample 2 is between 192.2 and 206 (kJ/mol), which is higher than sample 1, and 0.9 conversion is excluded due to the low energy received compared to the other data. The mean Ea is calculated and found to be more than sample 1, about 212.7 kJ/mol, and 10 is the standard deviation (STDEVA). Sample 1 has the lowest activation energy compared with sample 2. It means that the energy required for a chemical reaction to proceed is minimized.

Table 4. The calculated values of activation energy using different slope values for sample 1.

conversion	Ea (kJ/mol)
0.1	177.1
0.2	185.4
0.3	189.6
0.4	196.2
0.5	196.7
0.6	199.6
0.7	204.6
0.8	216.5
0.9	233.8
Mean Ea (kJ/mol)	195.7
STDEVA	12

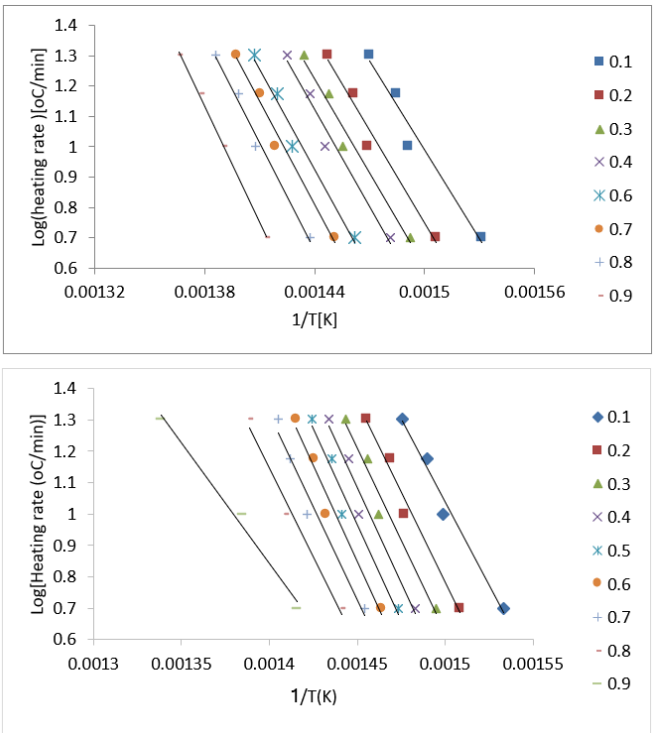

Figure 8. Linear fit plots for determination of activation energy through FWO method applied to (a) sample1 and (b) sample 2.

However, Table 5 demonstrated that the growth of Ea for sample 2 stopped at 0.6 conversions. Then it decreased at conversion values 0.7 and 0.8 with E_a values around 216 and 106 (kJ/mol), respectively. This reduction may be due to the reaction process being completed faster than before, and low energy is required.

Table 5. The calculated values of activation energy using different slope values for sample 2.

conversion	Ea (kJ/mol)
0.1	192.2
0.2	207.8
0.3	214.4
0.4	220.3
0.5	222.3
0.6	222.8
0.7	216.2
0.8	206
0.9	140

Mean Ea (kJ/mol)	212.7
STDEVA	10.4
	Without 0.9

4. Conclusions

NiO as nanoparticles were created using the sol-gel method with two different calcination approaches. The catalyst of NiO using the furnace and microwave are used to nucleate nanoparticles. The SEM analysis showed that the nanoparticles agglomerate, forming spherical-shaped particles for NiO. The TEM results reveal that the particle size was measured in the range of 45 to 95 nm. The NiO syntheses using microwave ve the lowest remaining weight percentage (5%)when mixed 1mg catalysis with 9 mg PET and the highest rate of reaction (20%). Also, it has a mean activation energy (195.7 kJ/mol) lesser than the furnace sample.

Funding

This research received no external funding.

Acknowledgments

Our appreciation to DARIS center for the support using the center's facilities

Conflicts of Interest

The authors declare no conflict of interest.

References

1. Abnisa, F.; Alaba, P.A. Recovery of liquid fuel from fossil-based solid wastes via pyrolysis technique: A review. *Journal of Environmental Chemical Engineering* **2021**, *9*, https://doi.org/10.1016/j.jece.2021.106593.
2. Al-Salem, S.M.; Karam, H.J.; Al-Wadi, M.H.; Alsamaq, S.; Jiang, G.; Wang, J.; Leeke, G.A. Thermal degradation kinetics of real-life reclaimed plastic solid waste (PSW) from an active landfill site: The mining of an unsanitary arid landfill. *Ain Shams Engineering Journal* **2021**, *12*, 983-993, https://doi.org/10.1016/j.asej.2020.05.011.
3. Anuar Sharuddin, S.D.; Abnisa, F.; Wan Daud, W.M.A.; Aroua, M.K. A review on pyrolysis of plastic wastes. *Energy Conversion and Management* **2016**, *115*, 308-326, https://doi.org/10.1016/j.enconman.2016.02.037.

4. Jahirul, M.I.; Rasul, M.G.; Schaller, D.; Khan, M.M.K.; Hasan, M.M.; Hazrat, M.A. Transport fuel from waste plastics pyrolysis – A review on technologies, challenges and opportunities. *Energy Conversion and Management* **2022**, *258*, https://doi.org/10.1016/j.enconman.2022.115451.
5. Osman, A.I.; Farrell, C.; Al-Muhtaseb, A.H.; Al-Fatesh, A.S.; Harrison, J.; Rooney, D.W. Pyrolysis kinetic modelling of abundant plastic waste (PET) and in-situ emission monitoring. *Environmental Sciences Europe* **2020**, *32*, 1-12, https://doi.org/10.1186/s12302-020-00390-x.
6. Kasar, P.; Sharma, D.K.; Ahmaruzzaman, M. Thermal and catalytic decomposition of waste plastics and its co-processing with petroleum residue through pyrolysis process. *Journal of Cleaner Production* **2020**, *265*, https://doi.org/10.1016/j.jclepro.2020.121639.
7. Zhang, H.; Zhou, X.-L.; Shao, L.-M.; Lü, F.; He, P.-J. Upcycling of PET waste into methane-rich gas and hierarchical porous carbon for high-performance supercapacitor by autogenic pressure pyrolysis and activation. *Science of The Total Environment* **2021**, *772*, https://doi.org/10.1016/j.scitotenv.2021.145309.
8. Huang, J.; Veksha, A.; Chan, W.P.; Giannis, A.; Lisak, G. Chemical recycling of plastic waste for sustainable material management: A prospective review on catalysts and processes. *Renewable and Sustainable Energy Reviews* **2022**, *154*, https://doi.org/10.1016/j.rser.2021.111866.
9. Singh, A.K.; Bedi, R.; Kaith, B.S. Composite materials based on recycled polyethylene terephthalate and their properties – A comprehensive review. *Composites Part B: Engineering* **2021**, *219*, https://doi.org/10.1016/j.compositesb.2021.108928.
10. Mishra, R.K.; Sahoo, A.; Mohanty, K. Pyrolysis kinetics and synergistic effect in co-pyrolysis of Samanea saman seeds and polyethylene terephthalate using thermogravimetric analyser. *Bioresource Technology* **2019**, *289*, https://doi.org/10.1016/j.biortech.2019.121608.
11. Honus, S.; Kumagai, S.; Fedorko, G.; Molnár, V.; Yoshioka, T. Pyrolysis gases produced from individual and mixed PE, PP, PS, PVC, and PET—Part I: Production and physical properties. *Fuel* **2018**, *221*, 346-360, https://doi.org/10.1016/j.fuel.2018.02.074.
12. Peng, Y.; Wang, Y.; Ke, L.; Dai, L.; Wu, Q.; Cobb, K.; Zeng, Y.; Zou, R.; Liu, Y.; Ruan, R. A review on catalytic pyrolysis of plastic wastes to high-value products. *Energy Conversion and Management* **2022**, *254*, https://doi.org/10.1016/j.enconman.2022.115243.
13. Wen, Y.; Zaini, I.N.; Wang, S.; Mu, W.; Jönsson, P.G.; Yang, W. Synergistic effect of the co-pyrolysis of cardboard and polyethylene: A kinetic and thermodynamic study. *Energy* **2021**, *229*, https://doi.org/10.1016/j.energy.2021.120693.
14. Dai, L.; Zhou, N.; Li, H.; Wang, Y.; Liu, Y.; Cobb, K.; Cheng, Y.; Lei, H.; Chen, P.; Ruan, R. Catalytic fast pyrolysis of low density polyethylene into naphtha with high selectivity by dual-catalyst tandem catalysis. *Science of The Total Environment* **2021**, *771*, https://doi.org/10.1016/j.scitotenv.2021.144995.
15. Luo, W.; Fan, Z.; Wan, J.; Hu, Q.; Dong, H.; Zhang, X.; Zhou, Z. Study on the reusability of kaolin as catalysts for catalytic pyrolysis of low-density polyethylene. *Fuel* **2021**, *302*, https://doi.org/10.1016/j.fuel.2021.121164.
16. Zhao, Z.; Abdo, S.M.A.; Wang, X.; Li, H.; Li, X.; Gao, X. Process intensification on co-pyrolysis of polyethylene terephthalate wastes and biomass via microwave energy: Synergetic effect and roles of microwave susceptor. *Journal of Analytical and Applied Pyrolysis* **2021**, *158*, http://doi.org/10.1016/j.jaap.2021.105239.
17. Qin, Z.-M.; Wang, P.-C.; Yang, R.; Chen, H.-B. Fast pyrolysis of silicones at low temperatures catalyzed by anatase titanium dioxide. *Polymer Degradation and Stability* **2020**, *182*, https://doi.org/10.1016/j.polymdegradstab.2020.109387.
18. Dineshkumar, M.; Begum, K.M.S.; Shrikar, B.; Ramanathan, A. Synthesis and characterization study of solid carbon biocatalyst produced from novel biomass char in a microwave pyrolysis. *Materials Today: Proceedings* **2021**, *46*, 9814-9819, https://doi.org/10.1016/j.matpr.2020.10.885.
19. Dai, L.; Wang, Y.; Liu, Y.; Ruan, R. Microwave-assisted pyrolysis of formic acid pretreated bamboo sawdust for bio-oil production. *Environmental Research* **2020**, *182*, https://doi.org/10.1016/j.envres.2019.108988.
20. Meher, S.K.; Justin, P.; Ranga Rao, G. Microwave-Mediated Synthesis for Improved Morphology and Pseudocapacitance Performance of Nickel Oxide. *ACS Applied Materials & Interfaces* **2011**, *3*, 2063-2073, https://doi.org/10.1021/am200294k.
21. Mohammed, S.A.; Al Amouri, L.; Yousif, E.; Abd Ali, A.; Mabood, F.; Abbas, H.F.; Alyaqoobi, S. Synthesis of NiO: V2O5 nanocomposite and its photocatalytic efficiency for methyl orange degradation. *Heliyon* **2018**, *4*, https://doi.org/10.1016/j.heliyon.2018.e00581.
22. Abd El-Lateef, H.M.; Khalaf, M.M.; Al-Omair, M.A.; Dao, V.-D.; Mohamed, I.M. Chemical synthesis of NiO nanostructure by surfactant-assisted sol–gel methodology for urea electrocatalytic oxidation. *Materials Letters* **2020**, *276*, https://doi.org/10.1016/j.matlet.2020.128192.
23. Alsurakji, I.H.; El-Qanni, A.; El-Hamouz, A.M.; Warad, I.; Odeh, Y. Thermogravimetric Kinetics Study of Scrap Tires Pyrolysis Using Silica Embedded With NiO and/or MgO Nanocatalysts. *Journal of Energy Resources Technology* **2021**, *143*, 1-15, https://doi.org/10.1115/1.4050814.
24. Joseph, S.; Mathew, B. Synthesis of silver nanoparticles by microwave irradiation and investigation of their catalytic activity. *Research Journal of Recent Sciences* **2014**, *3*, 185-191.

25. Kumagai, S.; Hasegawa, I.; Grause, G.; Kameda, T.; Yoshioka, T. Thermal decomposition of individual and mixed plastics in the presence of CaO or Ca (OH) 2. *Journal of analytical and applied pyrolysis* **2015**, *113*, 584-590, https://doi.org/10.1016/j.jaap.2015.04.004.
26. Orozco, S.; Alvarez, J.; Lopez, G.; Artetxe, M.; Bilbao, J.; Olazar, M. Pyrolysis of plastic wastes in a fountain confined conical spouted bed reactor: Determination of stable operating conditions. *Energy Conversion and Management* **2021**, *229*, https://doi.org/10.1016/j.enconman.2020.113768.
27. Safdari, M.-S.; Amini, E.; Weise, D.R.; Fletcher, T.H. Heating rate and temperature effects on pyrolysis products from live wildland fuels. *Fuel* **2019**, *242*, 295-304, https://doi.org/10.1016/j.fuel.2019.01.040.
28. Gebre, S.H.; Sendeku, M.G.; Bahri, M. Recent Trends in the Pyrolysis of Non-Degradable Waste Plastics. *ChemistryOpen* **2021**, *10*, 1202-1226, https://doi.org/10.1002/open.202100184.
29. Li, C.; Ataei, F.; Atashi, F.; Hu, X.; Gholizadeh, M. Catalytic pyrolysis of polyethylene terephthalate over zeolite catalyst: Characteristics of coke and the products. *International Journal of Energy Research* **2021**, *45*, 19028-19042, https://doi.org/10.1002/er.7078.
30. Liu, Y.; Fu, W.; Liu, T.; Zhang, Y.; Li, B. Microwave pyrolysis of polyethylene terephthalate (PET) plastic bottle sheets for energy recovery. *Journal of Analytical and Applied Pyrolysis* **2022**, *161*, https://doi.org/10.1016/j.jaap.2021.105414.
31. Poletto, M. Thermogravimetric analysis and kinetic study of pine wood pyrolysis. *Revista Ciência da Madeira (Brazilian Journal of Wood Science)* **2016**, *7*, http://dx.doi.org/10.12953/2177-6830/rcm.v7n2p111-118.